

Designing micro-patterned Ti films that survive up to 10% applied tensile strain

Noble C. Woo · Kunigunde Cherenack ·
Gerhard Tröster · Ralph Spolenak

Received: 27 April 2010 / Accepted: 26 May 2010 / Published online: 12 June 2010
© Springer-Verlag 2010

Abstract Reducing the strain in brittle device layers is critical in the fabrication of robust flexible electronic devices. In this study, the cracking behavior of micro-patterned 500-nm-thick Ti films was investigated via uniaxial tensile testing by in situ SEM and 4-point probe measurements. Both visual observations by SEM and 4-pt resistance measurements showed that strategically patterned oval holes, off-set and rotated by 45°, had a significant effect on limiting the extent of cracking, specifically, in preventing cracks from converging. Failure with regard to electrical conduction was delayed from less than 2% to more than 10% strain.

1 Introduction

Flexible electronics represent the next evolutionary development within the field of microelectronics and enable a wide range of novel applications including paper-like displays [1], smart textiles [2] and large-area sensor arrays [3]. In comparison to devices fabricated on rigid silicon or glass substrates, devices on flexible substrates may experience high mechanical strain, resulting in circuit failure due to device layer cracking.

Finite element studies have shown that ductile metal films which are well bonded to Kapton polyimide substrates can

be stretched well beyond their bulk rupture strain due to strain delocalization of the substrate [4] and researchers have measured tensile rupture strains for thin-film copper metal on Kapton substrates up to 50% and higher [5]. However, brittle device layers typically fail at around 2% strain [6] and have a probably unattainable theoretical strain limit (all bonds breaking at the same time) of roughly 10%. Therefore it is critical that the strain in brittle device layers is reduced below the value at which cracking is initiated. Methods of reducing the strain experienced by device layers include preventing the propagation of cracks through the device layers through nano-patterning [7, 8], reducing the strain in layers below the fracture limit of the material by patterning islands [9, 10] or shifting the critical device layers closer to the neutral bending plane [11, 12].

At high strains, crack nucleation saturates when the spacing between adjacent cracks (crack spacing) reaches equilibrium; multiple cracks interact over a critical length, the stress transfer length (STL), which is given by half the minimum crack spacing [13–17]. The STL is unique for a given material combination and thickness. The aim of this investigation is to find out whether patterning films with holes spaced at distances equal to or less than the STL is successful in stopping cracks from interacting and propagating through a brittle thin-film layer (or even prohibits new cracks from nucleating). We believe that certain geometrical patterns could also act to localize cracks at hole-edges and would therefore reduce or constrain layer cracking by geometrical means.

In this work, we investigate the fracture behavior of 500-nm-thick micro-patterned titanium (Ti) layers deposited on polyimide (Kapton® E) substrates. Although commonly used brittle device layers—such as SiN_x or Al₂O₃ dielectric layers in thin-film transistors—are more interesting from an application perspective, we decided to use a brittle metal

N.C. Woo · R. Spolenak (✉)
Laboratory for Nanometallurgy, Department of Materials, ETH
Zürich, Wolfgang-Pauli-Strasse 10, 8093 Zürich, Switzerland
e-mail: spolenak@mat.ethz.ch

N.C. Woo
e-mail: noble.woo@mat.ethz.ch

K. Cherenack · G. Tröster
Wearable Computing Lab, Institute for Electronics, ETH Zürich,
Gloriastrasse 35, 8092 Zürich, Switzerland

for this proof-of-concept research. The advantage to investigating cracking in a brittle metal is that changes in sample resistance versus applied strain can provide valuable information to interpret physical changes in the material caused by cracking. Therefore, Ti films were patterned with oval holes that were rotated by 45° and off-set along adjacent lines to make the cracking behavior insensitive to the chosen tensile direction. Patterning of metal layers significantly reduces the cracking behavior of the thin-film brittle layer and shows that this method can be used as a tool for fabricating strain-tolerant thin-film devices on flexible substrates.

2 Experimental procedure

The substrates used in our work were 50 μm -thick Kapton[®] E substrates from DuPont with a surface area of $7.6\text{ cm} \times 7.6\text{ cm}$. Brittle Ti films with a thickness of 500 nm were deposited onto the substrates using thermal evaporation. Preliminary measurements of these films gave a STL of $\sim 15\text{ }\mu\text{m}$ (half the minimum crack spacing), which was measured using the method described in [13–17]. The mask designed to pattern the Ti layers consists of oval-shaped holes that have a length of 18 μm and a width of 8 μm . Ovals are spaced apart by 40 μm in both the horizontal and vertical direction and ovals in alternate lines are flipped along the vertical axis by 45° and off-set by 20 μm . Therefore adjacent ovals (center to center) are separated by 28.3 μm at a 45° . The SEM images on the right-hand side in Fig. 2 show images taken of a patterned film at various stages of applied tensile strain. All substrates were cleaned by sonicating them in acetone and isopropanol for 10 minutes respectively, and were then pre-shrunk in a vacuum oven at 200°C for 24 hours to remove trapped residual solvents [18]. Two substrates were metalized with 500 nm of Ti (samples 1 and 2). The film thicknesses were confirmed using a Tencor Alpha-Step 500 profilometer. The metal layer on sample 1 was patterned with the oval-hole pattern and the metal layer on sample 2 was left unpatterned. Sample 1 was prepared for lift-off using standard photolithography as follows: first substrates were mounted temporarily on glass slides using a drop of water for adhesion, and were coated with hexamethyldisiloxane (HMDS) as an adhesion promoter and MA-N1420 negative photoresist from Microresist Technology at a spin speed of 3000 rpm for 30 seconds. Afterwards, the substrates were baked at 160°C for 120 seconds and exposed the photoresist at an energy density of 550 mJ/cm^2 at 365 nm using a mask loaded into a Karl Süss MA6 mask aligner. Exposed substrates were developed in MA-D533 developer for 150 seconds. Then we deposited 500 nm of Ti (sample 1) using a Univex 500 thermal evaporator. The metal pattern was then developed by sonicating the substrates in a bath of acetone for 5 min after which the surface was rinsed with iso-

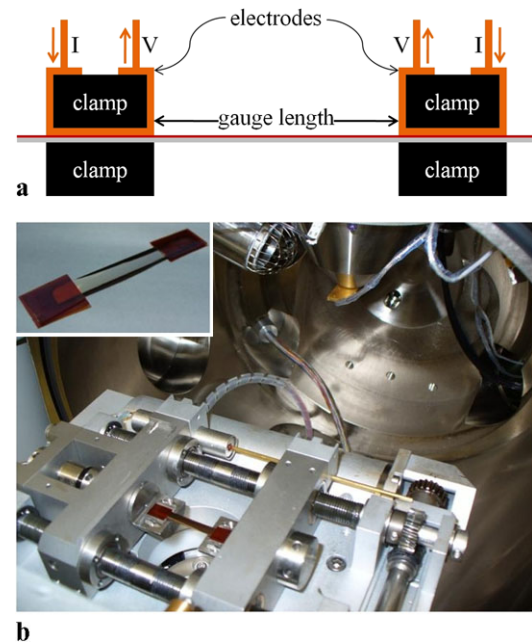


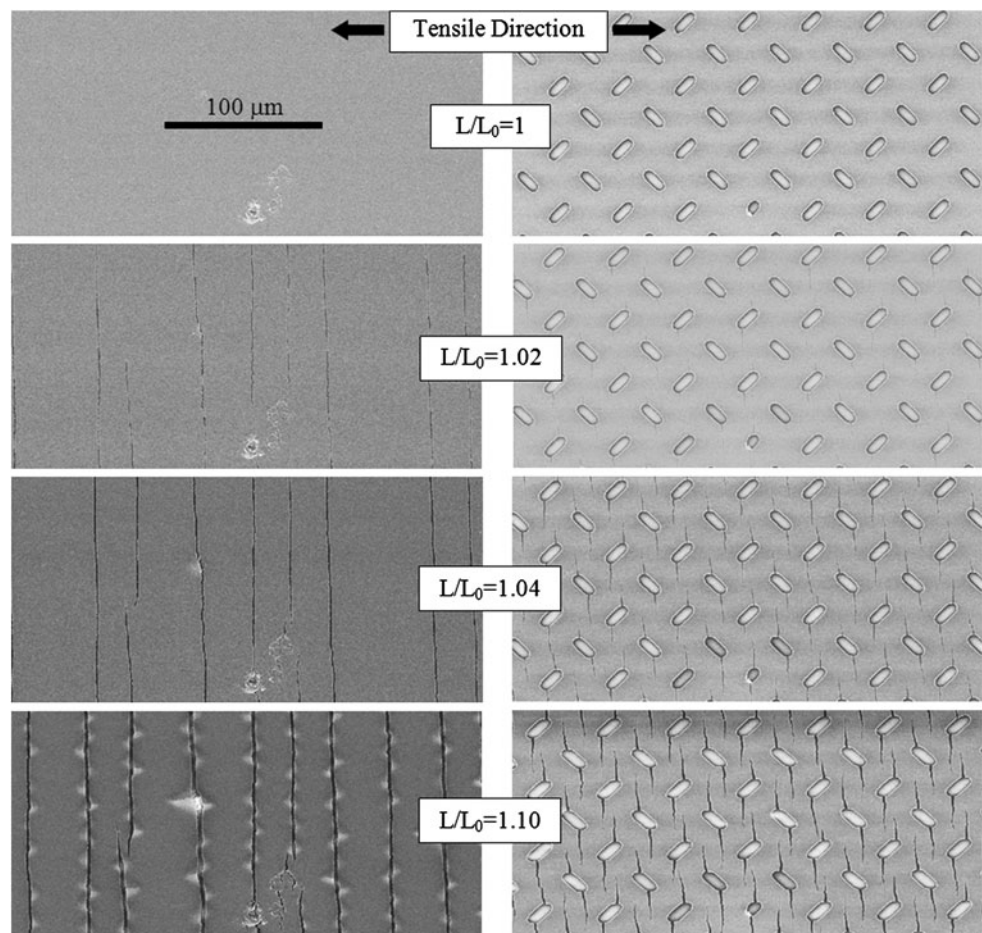
Fig. 1 The schematics of the tensile experiments: (a) the resistance measurement and (b) the tensile tester loaded inside the SEM including a mounted sample

propanol. Finally, we cut 4-mm wide samples from samples 1 and 2 for mechanical testing.

The local evolution of cracks as a function of applied strain can be observed using image analysis and the quantitative cracking behavior can be corroborated [15, 16]. Uniaxial mechanical tensile testing was carried out using a tensile tester (Kammrath and Weiss, Germany) on the patterned brittle Ti film and the unpatterned control film. Samples were loaded into the tensile tester so that the inner distance between the clamps, also referred to as the gauge length, was 20 mm (see Fig. 1(a)). To observe cracking behavior, tensile tests were carried out in situ using SEM (FEI Quanta 200 FEG, USA) and SEM images were acquired at a chosen location using the secondary electron detector. SEM images were obtained at successive strains and were used in image analysis to investigate local film fracture behavior, and to determine the onset of plasticity. Applied strains were determined from both the tensile tester displacements and from the SEM images. Figure 1(b) shows a sample loaded into the tensile tester, inside the SEM chamber.

Complementary to mechanical evaluation, electrical characterization was carried out to monitor cracking behavior qualitatively. Since this resistance is measured across the entire sample, the method allows real-time monitoring of electrical conduction throughout the sample, in contrast to the localized SEM method. In our work, we monitored electrical resistance as a function of continuous applied strain using a Kelvin (4-point probe) technique to carry out in situ resistance measurements during mechanical tensile strain-

Fig. 2 SEM images showing unpatterned and patterned 500-nm-thick Ti film surfaces for applied tensile strains at 0%, 2%, 4% and 10%. Images on the left column are from unpatterned Ti film. Images on the right side are from the patterned Ti film with oval holes rotated and off-set as shown. For the images shown, the tensile strain direction is horizontal



ing. Figure 2(a) shows a schematic of the in situ resistance measurement setup. Both data acquisition and straining were automated to reduce external interference from the experimenter. A LabView-based data acquisition system was automated to continuously measure resistance at 100-millisecond intervals at a pre-set tensile straining speed of 2 micrometers/second. This resulted in a strain-rate of 10^{-4} s^{-1} for a 20-mm gauge length. Of the four probes, the outer two supplied current using an independent current supply, while the inner two measured the voltage dropped across the sample. The gauge length was measured precisely to ensure accurate measurement of initial resistance.

3 Results and discussion

Figure 2 shows SEM images taken of unpatterned and patterned Ti samples at various applied tensile strains. The images in the left column are from the unpatterned Ti and those in the right column are from the patterned Ti. In these images, the tensile straining was in the horizontal direction, and therefore we see the formation of vertical cracks. For the unpatterned sample, cracks nucleate at defects and in-

stantaneously span the entire width of the sample. This occurs at strains less than 2%. Therefore, there should be no electrical conduction across the horizontal direction and in a device such long cracks would result in total device failure. In comparison, for patterned samples a percolation path was still found at strains of 10%.

From the 4-point probe measurements, we obtained the normalized change of resistance versus applied tensile strain for unpatterned and patterned samples, which is plotted in Fig. 3. The resistance of the metal line in our experiment, R , can be defined by $R = \rho L/A$ where ρ is the resistivity of the material, L is the length of current conduction path and A is the cross-sectional area perpendicular to the current flow. In the first approximation, the change in resistance is due to a change in the length L (typically equivalent to the sample length) and sample cross section A . The effect of elastic strain on resistivity (piezoresistivity) is neglected for metallic materials. In the first phase of a uniaxial test (region I in Fig. 3) the conducting material deforms elastically and a change in cross section A is due to Poisson's effect with a Poisson ratio of roughly one third for metallic materials. Upon further straining the conducting material reacts in one of the three ways, which are illustrated in the

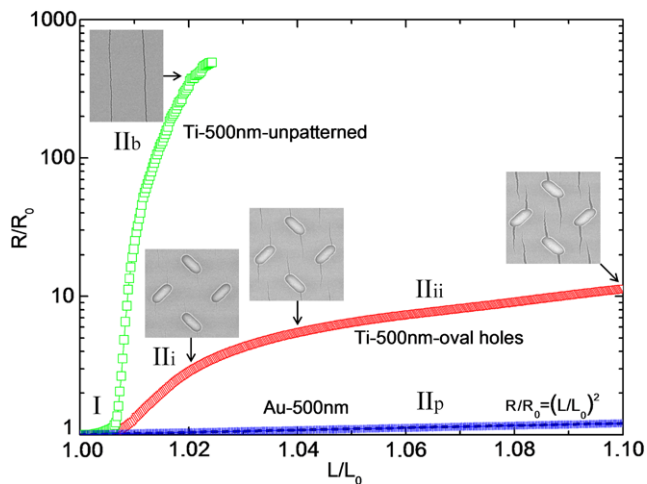


Fig. 3 Normalized resistance as a function of applied tensile strain of the unpatterned Ti film, the patterned Ti film, unpatterned Au film and the ideal change in resistance (*dashed line*) are plotted. For all films, region I—the elastic regime up to 0.7% strains—follows ideal change. Region II's represent different deformation behaviors; Au film shows ideal plastic deformation (IIp) according to volume conservation without cracking; Unpatterned Ti failed with brittle fracture (IIb) controlled by crack nucleation (cracks span the entire width once nucleated); and lastly, 2 regions for patterned Ti film—IIi represents crack propagation which leads to reduction in effective cross-sectional area for electrical conduction and IIii represents crack opening/widening in addition to crack propagation observed in III. Indeed, region IIIii has an additional factor in increasing effective conduction path with percolation path circumventing the cracks

following: plastic deformation (region IIp), brittle cracking (region IIb), and crack-pattern interaction (regions IIIi and IIIii in Fig. 3).

The ideal resistance change for a plastically deforming crack-free sample assumes volume conservation which is equivalent to a Poisson's ratio of one half. It is modeled as $R/R_0 = (L/L_0)^2$ where R/R_0 is the normalized resistance and L/L_0 is the relative length change [5]. This function was overlapped to the resistance change of a 500-nm-thick Au film, which stayed crack-free over the strain range of interest. The resistance change of the Au sample followed the theoretical curve exactly. Any deviation of plotted resistance change from the ideal line in Fig. 3 is therefore indicative of cracking.

In region I (up to 0.7% strain), all films exhibit elastic behavior. In region II, however, different deformation behavior can be found. The unpatterned Ti failed by brittle fracture (IIb) dominated by crack nucleation as each crack instantaneously spanned the entire width of the film resulting in strong resistance increases (note that the resistance scale is logarithmic). For example, at 2% strain, the normalized resistance of unpatterned Ti is 400 times that of Au. Patterned Ti films, however, only showed a 3 fold increase and demonstrated a totally different cracking behavior. In fact, Fig. 3 shows that patterned Ti film has 2 types of fracture behaviors: region IIIi results from crack nucleation and propagation

that leads to a decrease in the effective cross-sectional area A (relative to the line-of-sight conduction path) for electrical conduction. In region IIIii, the line-of-sight path is closed and further crack growth results in an increase of the length of the conduction path L . In addition part of the sample strain is accommodated by significant crack opening (compare the widening of cracks in the insets in Fig. 3). The latter two mechanisms jointly lead to a reduction in the strain sensitivity of the resistance between region IIIi and region IIIii.

The sensitivity can be quantified by setting it into relation with the plastically deforming (ideal) gold curve. It amounts to $A_{\text{ideal}}/A_{\text{patternedTi}} = R_{\text{patternedTi}}/R_{\text{ideal}} \approx 145$ per unit strain for region IIIi and 95 per unit strain for region IIIii. In the latter, the overlapping arrangement of cracks prevents them from joining and results in a percolation path at strains of greater than 10%. The sensitivity of the unpatterned Ti film (region IIb) is close to infinity.

In general, the strong improvement in strain resistance for the patterned Ti is due to the placement and orientation of the oval-shaped holes in the film which effectively limited crack propagation and converging. In particular, by offsetting oval holes in adjacent lines and rotating by 45°, we prevented multiple cracks from converging, regardless of the tensile direction, and allowed percolation path to exist.

4 Conclusion

The cracking behavior of micro-patterned brittle Ti films was investigated via uniaxial tensile straining by in situ visual inspection of SEM images taken during strain application and by 4-point probe measurements to extract the normalized change in sample resistance versus applied strain. Visual observation of SEM images allowed quantitative determination of cracking as a function of applied strain. The sequence of images clearly shows that strategically patterned oval-shaped holes have a significant effect in reducing cracking behavior. The patterned oval holes prevented cracks from continuing across the width of the sample, and therefore are able to prevent total loss of conduction. In addition, oval holes that were rotated by 45° and off-set in adjacent lines prevented multiple cracks from converging. The normalized resistance curves as a function of strain also shows the same positive effect of having patterned holes on crack propagation. The slower rise in resistance of the patterned film compared to the unpatterned one indicated the existence of percolation path within the film, allowing conduction to take place. This allows delaying failure of electrical conduction in brittle thin films from less than 2% to more than 10% strain. This is an improvement of a factor of 5 and may provide the necessary improvements in device robustness to fabricate truly robust flexible thin-film devices. Future experiments will involve application of this

method to more common brittle device layers such as SiN_x and ultimately achieve more strain-resistant thin-film devices through micro-patterning of brittle device layers.

Acknowledgements This work has been financed by the Swiss National Science Foundation within the Nano-Tera.ch initiative. Noble C. Woo would like to thank Entwicklungsfonds Seltene Metalle (ESM) Foundation for his postdoctoral fellowship. In addition, authors would like to acknowledge the Electron Microscopy Center of ETH Zurich (EMEZ) for supporting in situ SEM works and thank Dr. Christopher Simone from DuPont for their support, Stephan Frank for detail discussion of earlier pattern designs and Niko Münzenrieder for lithography.

References

1. G.P. Crawford, *Flexible Flat Panel Displays* (Wiley, Chichester, 2005), pp. 263–282
2. E. Bonderover, S. Wagner, A woven inverter circuit for e-textile applications. *IEEE Electron Device Lett.* **25**(5), 295–297 (2004)
3. T. Someya, T. Sekitani, S. Iba, Y. Kato, H. Kawaguchi, T. Sakurai, A large-area, flexible pressure sensor matrix with organic field-effect transistors for artificial skin applications. *Proc. Natl. Acad. Sci. USA* **101**(27), 9966–9970 (2004)
4. T. Li, Z.Y. Huang, Z.C. Xi, S.P. Lacour, S. Wagner, Z. Suo, Delocalizing strain in a thin metal film on a polymer substrate. *Mech. Mater.* **37**, 261–273 (2005)
5. N. Lu, X. Wang, Z. Suo, J. Vlassak, Metal films on polymer substrates stretched beyond 50%. *Appl. Phys. Lett.* **91**, 221909 (2007)
6. Z. Suo, E.Y. Ma, H. Gleskova, S. Wagner, Mechanics of rollable and foldable film-on-foil electronics. *Appl. Phys. Lett.* **74**(8), 1177–1179 (1999)
7. P. Mandlik, S.P. Lacour, J.W. Li, S.Y. Chou, S. Wagner, Fully elastic interconnects on nanopatterned elastomeric substrates. *IEEE Electron Device Lett.* **27**(8), 650–652 (2006)
8. P. Ekkels, R.W. Tjerkstra, G.J.M. Krijnen, J.W. Berenschot, J. Brugger, M.C. Elwenspoek, Fabrication of functional structures on thin silicon nitride membranes. *Microelectron. Eng.* **67–68**(1), 422–429 (2003)
9. P.I. Hsu, H. Gleskova, M. Huang, Z. Suo, S. Wagner, J.C. Sturm, Amorphous Si TFTs on plastically deformed spherical domes. *J. Non-Cryst. Solids* **299–302**(2), 1355–1359 (2002)
10. S. Lacour, J. Jones, S. Wagner, T. Li, Z. Suo, Stretchable interconnects for elastic electronics surfaces. *Proc. IEEE* **93**(8), 1459–1467 (2005)
11. W. Christiaens, T. Loeher, B. Pahl, M. Feil, B. Vandevelde, J. Vanfleteren, Embedding and assembly of ultrathin chips in multilayer flex boards. *Circuit World* **34**(3), 3–8 (2008)
12. D. Verebelyi, E. Harley, J. Scudiere, A. Otto, U. Schoop, C. Thieme, N. Rupich, A. Maloyemoff, Practical neutral-axis conductor geometries for coated conductor composite wire. *Supercond. Sci. Technol.* **16**, 1158–1161 (2003)
13. U.A. Handge, Y. Leterrier, G. Rochat, I.M. Sokolov, A. Blumen, Two scaling domains in multiple cracking phenomena. *Phys. Rev. E* **62**(6), 7807–7810 (2000)
14. U.A. Handge, Analysis of a shear-lag model with nonlinear elastic stress transfer for sequential cracking of polymer coatings. *J. Mater. Sci.* **37**, 4775–4782 (2002)
15. M. Heinrich, P. Gruber, S. Orso, U.A. Handge, R. Spolenak, Dimensional control of brittle nanoplatelets: a statistical analysis of a thin film cracking approach. *Nano Lett.* **6**(9), 2026–2030 (2006)
16. S. Frank, U.A. Handge, S. Olliges, R. Spolenak, The relationship between thin film fragmentation and buckle formation: synchrotron-based in situ studies and two-dimensional stress analysis. *Acta Mater.* **57**, 1442–1453 (2009)
17. Z.C. Xia, J.W. Hutchinson, Crack patterns in thin films. *J. Mech. Phys. Solids* **48**, 1107–1131 (2000)
18. [Online] http://www2.dupont.com/Kapton/en_US/, downloaded January 2010